Non-Fermi Liquid Behavior from Critical Fermi Surface Fluctuations

Walter METZNER[1] and Luca DELL'ANNA[2]

[1] *Max-Planck-Institute for Solid State Research, D-70569 Stuttgart, Germany*
[2] *International School for Advanced Studies (SISSA), I-34014 Trieste, Italy*

Interactions in Fermi systems can generate a Pomeranchuk instability leading to orientational symmetry breaking, that is, nematic order. In a metallic system close to such an instability the Fermi surface is easily deformed by anisotropic perturbations and exhibits enhanced collective fluctuations. We analyze fluctuation effects in the quantum critical regime near a d-wave Pomeranchuk instability in two dimensions. Density correlations with a d-wave form factor and the dynamical forward scattering interaction diverge near the instability. The singular forward scattering leads to large self-energy contributions, which destroy Fermi liquid behavior over the whole Fermi surface except at "cold spots" on the Brillouin zone diagonal. The decay rate of single-particle excitations, which is related to the width of the peaks in the spectral function, exceeds the excitation energy in the low-energy limit. The dispersion of the spectra flattens strongly near those portions of the Fermi surface which are remote from the zone diagonal. The decay rate for DC transport is linear in temperature except at the cold spots. We discuss the possible relevance of d-wave Fermi surface fluctuations for the "strange metal" behavior observed in the normal phase of cuprates.

§1. Introduction

Electron-electron interactions can generate a spontaneous breaking of the rotation symmetry of an itinerant electron system without breaking translation invariance. From a Fermi liquid viewpoint, such an instability is driven by forward scattering interactions and leads to a symmetry breaking deformation of the Fermi surface. In isotropic three-dimensional Fermi liquids this instability sets in when Landau parameters exceed certain critical negative values, as derived already in 1958 by Pomeranchuk.[1)] We therefore refer to instabilities leading to a symmetry-breaking Fermi surface deformation as *"Pomeranchuk instabilities"*, extending the notion also to anisotropic systems (on a lattice), two-dimensional systems, and non-Fermi liquid metals.

Pomeranchuk instabilities leading to symmetry-breaking deformations of the Fermi surface in interacting electron systems have attracted considerable interest in the last few years. Effective interactions favoring a Pomeranchuk instability with $d_{x^2-y^2}$-wave symmetry have been found in the two most intensively studied models for cuprate superconductors, that is, the two-dimensional t-J[2)] and Hubbard[3),4)] model. The corresponding Fermi surface deformations are illustrated in Fig. 1. These models thus exhibit enhanced *"nematic"* correlations, as usually discussed in the context of fluctuating stripe order.[5)] Signatures for incipient nematic order with d-wave symmetry have been observed in several cuprate materials.[6)] In particular, nematic correlations close to a d-wave Pomeranchuk instability provide an appealing explanation for the relatively strong in-plane anisotropy observed in the magnetic excitation spectrum of $YBa_2Cu_3O_y$.[7),8)] A spin dependent Pomeranchuk instability

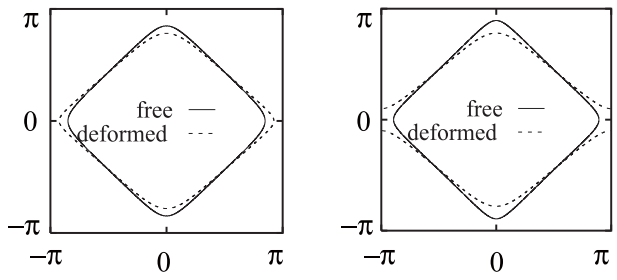

Fig. 1. Schematic illustration of Fermi surface deformations with $d_{x^2-y^2}$-symmetry on a square lattice; the deformed Fermi surface may be closed (left) or open (right).

was recently invoked to characterize a new phase observed in ultrapure crystals of the layered ruthenate metal $Sr_3Ru_2O_7$,[9] and also to account for a puzzling phase transition in URu_2Si_2.[10]

A Pomeranchuk instability usually competes with other instabilities, but can also coexist with other symmetry breaking order. For example, in the two dimensional Hubbard model with a sizable next-to-nearest neighbor hopping and an electron density near van Hove filling a superconducting ground state with a d-wave deformed Fermi surface can be established.[11] The competition between d-wave superconductivity and a d-wave Pomeranchuk instability has been analyzed more comprehensively in a phenomenological mean-field model.[12] Superconducting nematic states have also been included in a general classification of possible symmetry breaking patterns.[13] In the present article, however, we will focus on symmetry breaking Fermi surface deformations in an otherwise normal state.

Electron systems in the vicinity of a Pomeranchuk instability exhibit peculiar properties due to a *"soft" Fermi surface*, which can be easily deformed by anisotropic perturbations. Critical fluctuations near a Pomeranchuk quantum critical point provide an interesting route to *non-Fermi liquid behavior* in two dimensions.[14),15] For a d-wave Pomeranchuk instability in an electron system on a square lattice the singular part of the electronic self-energy is proportional to $d_{\boldsymbol{k}}^2$, where $d_{\boldsymbol{k}}$ is a form factor with d-wave symmetry.[15] At the quantum critical point, the real and imaginary parts of the self-energy scale as $|\omega|^{2/3}$ with energy. This leads to a complete destruction of quasi-particles near the Fermi surface except for the "cold spots" on the Brillouin zone diagonal, where the form factor $d_{\boldsymbol{k}}$ vanishes. In the quantum critical regime at $T > 0$ the self-energy consists of a "classical" and a "quantum" part with very different dependences on T and ω. The classical part, which is due to classical fluctuations, dominates at $\omega = 0$ and yields a contribution proportional to $\sqrt{T/\log T}$ to the imaginary part of the self-energy on the Fermi surface.[16] The momentum dependent transport decay rate $\gamma_{\boldsymbol{k}}^{\rm tr}(T)$ is *linear* in temperature for all momenta on the Fermi surface except at the cold spots on the Brillouin zone diagonal.[17] Adding a conventional T^2-term to $\gamma_{\boldsymbol{k}}^{\rm tr}(T)$ yields an overall resistivity $\rho(T)$ proportional to $T^{3/2}$ at low temperatures. In the presence of impurities, the residual resistivity at zero temperature is approached linearly.

In the following, we review the derivation of the above-mentioned non-Fermi liquid properties near a Pomeranchuk quantum critical point.

§2. Forward scattering model

Fluctuation effects in the vicinity of a Pomeranchuk instability are captured by a phenomenological lattice model with an interaction which drives a Fermi surface symmetry breaking, but no other instability. The model Hamiltonian[15] reads

$$H = \sum_{\boldsymbol{k},\sigma} \epsilon_{\boldsymbol{k}}\, n_{\boldsymbol{k}\sigma} + \frac{1}{2V} \sum_{\boldsymbol{k},\boldsymbol{k}',\boldsymbol{q}} f_{\boldsymbol{k}\boldsymbol{k}'}(\boldsymbol{q})\, n_{\boldsymbol{k}}(\boldsymbol{q})\, n_{\boldsymbol{k}'}(-\boldsymbol{q}) \;, \tag{2·1}$$

where $\epsilon_{\boldsymbol{k}}$ is a single-particle dispersion, $n_{\boldsymbol{k}}(\boldsymbol{q}) = \sum_\sigma c^\dagger_{\boldsymbol{k}-\boldsymbol{q}/2,\sigma} c_{\boldsymbol{k}+\boldsymbol{q}/2,\sigma}$, and V is the volume of the system. As the Pomeranchuk instability is driven by interactions with vanishing momentum transfers (forward scattering), we choose a function $f_{\boldsymbol{k}\boldsymbol{k}'}(\boldsymbol{q})$ which contributes only for small momenta $\boldsymbol{q}$, and refer to the above model as the "*f-model*". Obviously this model is adequate only if the Pomeranchuk instability dominates over other instabilities and fluctuations in the system. Otherwise it would have to be supplemented by interactions with large momentum transfers.

For a simplified treatment, which however fully captures the essential physics, we choose an interaction of the form

$$f_{\boldsymbol{k}\boldsymbol{k}'}(\boldsymbol{q}) = u(\boldsymbol{q}) + g(\boldsymbol{q})\, d_{\boldsymbol{k}}\, d_{\boldsymbol{k}'} \tag{2·2}$$

with $u(\boldsymbol{q}) \geq 0$ and $g(\boldsymbol{q}) < 0$, and a form factor $d_{\boldsymbol{k}}$ with $d_{x^2-y^2}$ symmetry, such as $d_{\boldsymbol{k}} = \cos k_x - \cos k_y$. The coupling functions $u(\boldsymbol{q})$ and $g(\boldsymbol{q})$ vanish if $|\boldsymbol{q}|$ exceeds a certain small momentum cutoff Λ. This ansatz mimics the effective interaction in the forward scattering channel as obtained from renormalization group calculations[3] and perturbation theory[18] for the two-dimensional Hubbard model near van Hove filling. The uniform term originates directly from the repulsion between electrons. The d-wave term drives the Pomeranchuk instability.

The mean-field solution of the f-model has been studied in detail for various choices of parameters.[19–21] In the plane spanned by the chemical potential μ and temperature T the symmetry-broken phase is formed below a dome-shaped transition line $T_c(\mu)$ with a maximal transition temperature near van Hove filling. The phase transition is typically first order near the edges of the transition line, that is where T_c is relatively low, and always second order near its center.[20] The two tricritical points at the ends of the second order transition line can be shifted to lower temperatures by a sizable uniform repulsion u included in $f_{\boldsymbol{k}\boldsymbol{k}'}$.[21] For a suitable choice of hopping and interaction parameters, one of the first order edges is suppressed completely such that a quantum critical point is realized. Although quantum critical points are usually prevented by first order transitions at low temperatures in the f-model, the Fermi surface is nevertheless already very soft near the transition, such that fluctuations can be expected to be important.[21]

§3. Effective interaction

We now derive and analyze the dynamical effective interaction for the f-model, which is closely related to the dynamical *d-wave density correlation* function

$$N_d(\boldsymbol{q},\nu) = -i\int_0^\infty dt\; e^{i\nu t}\,\langle[n_d(\boldsymbol{q},t), n_d(-\boldsymbol{q},0)]\rangle\;. \tag{3·1}$$

The d-wave density fluctuation operator is defined as

$$n_d(\boldsymbol{q}) = \sum_{\boldsymbol{k}} d_{\boldsymbol{k}}\, n_{\boldsymbol{k}}(\boldsymbol{q})\;, \tag{3·2}$$

and $n_d(\boldsymbol{q},t)$ is the corresponding time-dependent operator in the Heisenberg picture. We first analyze $N_d(\boldsymbol{q},\nu)$ and the effective interaction within the random phase approximation (RPA), and subsequently discuss higher order corrections.

The RPA result for the d-wave density correlation function in the f-model reads

$$N_d(\boldsymbol{q},\nu) = \frac{\Pi_d^0(\boldsymbol{q},\nu)}{1-g(\boldsymbol{q})\,\Pi_d^0(\boldsymbol{q},\nu)} \tag{3·3}$$

with the bare d-wave polarization function

$$\Pi_d^0(\boldsymbol{q},\nu) = -\int \frac{d^2k}{(2\pi)^2}\,\frac{f(\epsilon_{\boldsymbol{k}+\boldsymbol{q}/2}-\mu) - f(\epsilon_{\boldsymbol{k}-\boldsymbol{q}/2}-\mu)}{\nu+i0^+-(\epsilon_{\boldsymbol{k}+\boldsymbol{q}/2}-\epsilon_{\boldsymbol{k}-\boldsymbol{q}/2})}\; d_{\boldsymbol{k}}^2\;. \tag{3·4}$$

The coupling $u(\boldsymbol{q})$ does not enter here because mixed polarization functions with a constant and a d-wave vertex vanish for small $\boldsymbol{q}$.

The RPA effective interaction is defined by the series of bubble chain diagrams sketched in Fig. 2, yielding

$$\Gamma_{\boldsymbol{k}\boldsymbol{k}'}(\boldsymbol{q},\nu) = \frac{u(\boldsymbol{q})}{1-u(\boldsymbol{q})\,\Pi^0(\boldsymbol{q},\nu)} \;+\; \frac{g(\boldsymbol{q})}{1-g(\boldsymbol{q})\,\Pi_d^0(\boldsymbol{q},\nu)}\, d_{\boldsymbol{k}}\, d_{\boldsymbol{k}'}\;, \tag{3·5}$$

where $\Pi^0(\boldsymbol{q},\nu)$ is the usual (s-wave) bare polarization function.

Close to the Pomeranchuk instability the denominator $1-g(\boldsymbol{q})\,\Pi_d^0(\boldsymbol{q},\nu)$ in Eqs. (3·3) and (3·5) becomes very small for $\boldsymbol{q}\to\boldsymbol{0}$ and $\nu\to 0$, if ν vanishes faster than $\boldsymbol{q}$, while $1-u(\boldsymbol{q})\,\Pi^0(\boldsymbol{q},\nu)$ remains of order one or even larger. The effective interaction is then dominated by the second term in Eq. (3·5), and can be written as

$$\Gamma_{\boldsymbol{k}\boldsymbol{k}'}(\boldsymbol{q},\nu) = g\, S_d(\boldsymbol{q},\nu)\, d_{\boldsymbol{k}}\, d_{\boldsymbol{k}'} \tag{3·6}$$

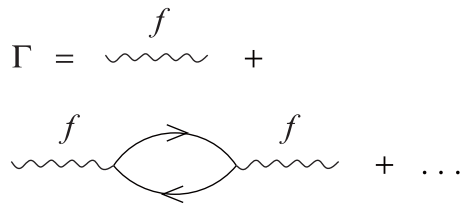

Fig. 2. Feynman diagrams contributing to the dynamical effective interaction Γ.

with $g = g(\mathbf{0})$ and the *"dynamical Stoner factor"*

$$S_d(\boldsymbol{q},\nu) = \frac{1}{1 - g(\boldsymbol{q})\, \Pi_d^0(\boldsymbol{q},\nu)} \; . \tag{3·7}$$

The d-wave density correlation function $N_d(\boldsymbol{q},\nu)$ is also proportional to $S_d(\boldsymbol{q},\nu)$. In case of a second order phase transition, the static Stoner factor

$$S_d = \lim_{\boldsymbol{q}\to 0} \lim_{\nu\to 0} S_d(\boldsymbol{q},\nu) \tag{3·8}$$

diverges on the transition line. Near the first order transition obtained typically for low temperatures in the mean-field solution of the f-model, S_d is still strongly enhanced.[21)]

Within RPA, the dynamical d-wave density fluctuations near the Pomeranchuk instability and the corresponding singularity of the effective interaction are determined by the asymptotic behavior of the d-wave polarization function $\Pi_d^0(\boldsymbol{q},\nu)$. Expanding $\Pi_d^0(\boldsymbol{q},\nu)$ for small $\boldsymbol{q}$ and ν with small $\nu/|\boldsymbol{q}|$, one obtains[16)]

$$\Pi_d^0(\boldsymbol{q},\nu) = a_1 + a_2\, |\boldsymbol{q}|^2 - i b(\hat{\boldsymbol{q}}) \frac{\nu}{|\boldsymbol{q}|} + \dots \; . \tag{3·9}$$

The coefficient a_1 is always negative and can be written as

$$a_1 = \int d\epsilon\, f'(\epsilon - \mu)\, N_{d^2}(\epsilon) \; , \tag{3·10}$$

where f is the Fermi function and $N_{d^2}(\epsilon) = \int \frac{d^2p}{(2\pi)^2}\, \delta(\epsilon - \epsilon_{\boldsymbol{p}})\, d_{\boldsymbol{p}}^2$ a weighted density of states. The sign of a_2 depends on the dispersion $\epsilon_{\boldsymbol{k}}$ and the precise form of $d_{\boldsymbol{k}}$. The coefficient $b(\hat{\boldsymbol{q}})$ is always positive and depends on the orientation of $\boldsymbol{q}$, as indicated by the unit vector $\hat{\boldsymbol{q}}$ in the argument.

Guided by the RPA result, but envisaging already corrections beyond RPA, we parametrize the dynamical Stoner factor for small $\boldsymbol{q}$ and ν, with $\nu/|\boldsymbol{q}|$ also small, as follows:

$$S_d(\boldsymbol{q},\nu) = \frac{1}{(\xi_0/\xi)^2 + \xi_0^2 |\boldsymbol{q}|^2 - i \frac{\nu}{c(\hat{\boldsymbol{q}})|\boldsymbol{q}|}} \; . \tag{3·11}$$

Within RPA, the length scales ξ_0 and ξ and the velocity $c(\hat{\boldsymbol{q}})$ are related in a simple fashion to the expansion coefficients of Π_d^0 and the coupling function $g(\boldsymbol{q})$. Expanding $g(\boldsymbol{q}) = g + g_2 |\boldsymbol{q}|^2 + \dots$ for small $\boldsymbol{q}$, we get

$$\xi_0^2 = -g\, a_2 - g_2\, a_1 \; , \tag{3·12}$$

$$(\xi_0/\xi)^2 = S_d^{-1} = 1 - g\, a_1 \; , \tag{3·13}$$

$$c(\hat{\boldsymbol{q}}) = -\frac{1}{g\, b(\hat{\boldsymbol{q}})} \; . \tag{3·14}$$

For $g < 0$ the velocity $c(\hat{\boldsymbol{q}})$ is positive. The static Stoner factor S_d diverges at the Pomeranchuk transition, if it is continuous, and the correlation length ξ diverges

accordingly as $\sqrt{S_d}$. The relation for ξ_0 is applicable only if the right-hand side is positive. This is guaranteed if we restrict ourselves to systems where the Pomeranchuk transition is the leading instability. For $-g\,a_2 - g_2\,a_1 < 0$ a charge density wave instability with a wave vector $\boldsymbol{q} \neq \boldsymbol{0}$ would set in first. The parameters ξ_0 and $c(\hat{\boldsymbol{q}})$ remain finite at the Pomeranchuk transition and do not vary much around it. The correlation length $\xi(\delta, T)$ near the transition depends sensitively on control parameters δ, such as the chemical potential, and on the temperature. If the transition is continuous, $\xi(\delta, T)$ diverges for $T \to T_c(\delta)$. Within the RPA, $\xi(\delta, T)$ diverges as $(T - T_c)^{-1/2}$ if $T_c(\delta) > 0$, and as T^{-1} if δ is tuned to a quantum critical point δ_c.

For small $\boldsymbol{q}$ and ν, with $\nu/|\boldsymbol{q}|$ also small, the d-wave density correlation function can be written as $N_d(\boldsymbol{q}, \nu) = -\kappa_d^0\, S_d(\boldsymbol{q}, \nu)$, where $\kappa_d^0 = -\lim_{\boldsymbol{q}\to\boldsymbol{0}} \lim_{\nu\to 0} \mathit{\Pi}_d^0(\boldsymbol{q}, \nu)$ is the non-interacting d-wave compressibility.[21)]

We now discuss corrections due to contributions not captured by the RPA. The exact density correlation function $N_d(\boldsymbol{q}, \nu)$ can be written in the form of Eq. (3·3), with the full polarization function $\mathit{\Pi}_d(\boldsymbol{q}, \nu)$, which is dressed by interactions, instead of the bare one. Similarly, the full effective interaction is given by Eq. (3·5) with dressed polarization functions $\mathit{\Pi}(\boldsymbol{q}, \nu)$ and $\mathit{\Pi}_d(\boldsymbol{q}, \nu)$. Close to a continuous phase transition two types of interaction corrections can be distinguished, namely regular interactions, which remain finite at the transition, and singular effective interactions associated with large order parameter fluctuations, which diverge.

Corrections to the RPA and corresponding subleading corrections to Fermi liquid behavior due to regular interactions, in a generic stable Fermi liquid regime, have been analyzed carefully in the last few years.[22)] The low energy behavior of most quantities receives non-analytic corrections to Fermi liquid behavior in dimensions $d \leq 3$. For example, in two dimensions the spin susceptibility varies as $|\boldsymbol{q}|$ instead of $|\boldsymbol{q}|^2$ for small $\boldsymbol{q}$ at $T = 0$. However, the charge susceptibility for small $\boldsymbol{q}$ remains unaffected. In this case non-analytic contributions appearing on the level of single Feynman diagrams cancel systematically when all relevant diagrams at a certain order are summed.[22)] A simple argument establishing the cancellation of non-analytic corrections for the charge susceptibility can be readily extended to our case of a d-wave density instead of the conventional density operator:[23)] A perturbing field coupling to the d-wave density operator does not alter the singularities in the polarization function at $\boldsymbol{q} = \boldsymbol{0}$ and $\boldsymbol{q} = 2\boldsymbol{k}_F$. Hence, corrections due to regular interactions may shift the parameters with respect to the RPA result for $N_d(\boldsymbol{q}, \nu)$ and $\mathit{\Gamma}_{\boldsymbol{k}\boldsymbol{k}'}(\boldsymbol{q}, \nu)$, but they do not yield any qualitative changes. Within the f-model, one such correction appears already on the mean-field level: the u-term in $f_{\boldsymbol{k}\boldsymbol{k}'}(\boldsymbol{q})$ generates a constant (momentum-independent) Hartree self-energy correction, which renormalizes the relation between μ and the density.[21)]

Near a continuous phase transition, order parameter correlations can be strongly modified with respect to the mean-field or RPA result. These fluctuation effects are most naturally treated by a renormalization group analysis of an effective field theory, where the order parameter fluctuations are represented by a bosonic field. The propagator of that field corresponds to the order parameter correlation function, that is to $N_d(\boldsymbol{q}, \nu)$ in our case. The singular effective interaction between electrons, which is generated by large order parameter fluctuations, is then mediated by the

bosonic field. In the bosonic representation, corrections to the RPA result for the order parameter correlations are due to interactions of the Bose field. Close to a continuous Pomeranchuk transition at finite T_c these terms are relevant and lead to the classical non-Gaussian asymptotic behavior of the Ising universality class in two dimensions. We will focus on the behavior in the *quantum* critical regime near the zero temperature critical point at $\delta = \delta_c$. In that regime the upper critical dimension separating Gaussian from non-Gaussian behavior is $d_c = 4 - z$, where z is the dynamical exponent.[24] In our case of a charge instability at $\boldsymbol{q} = \boldsymbol{0}$ one has $z = 3$, in complete analogy to the ferromagnetic quantum critical point in itinerant electron systems.[24] Hence we have $d_c = 1$, while the dimensionality of our system is two, such that Gaussian behavior is stable. However, as first pointed out by Millis,[25] the irrelevant quartic interaction of the order parameter fluctuations changes the temperature dependence of the correlation length near the quantum critical point completely compared to the RPA result. In particular, in a two-dimensional system with $z = 3$, the correlation length at δ_c behaves as[25]

$$\xi(\delta_c, T) \propto (T\,|\log T|)^{-1/2} \tag{3·15}$$

instead of the naive T^{-1}-divergence. Also the dependence of the transition temperature T_c on the control parameter is strongly affected by interactions. Near the quantum critical point, the condition $\xi^{-1} = 0$ yields an almost linear relation between the control parameter and the transition temperature,[26] $\delta - \delta_c \propto T_c \log T_c$, in agreement with estimates from the Ginzburg criterion.[25]

In summary, near the Pomeranchuk instability the electrons interact via a singular effective interaction of the form[15),16)]

$$\Gamma_{\boldsymbol{k}\boldsymbol{k}'}(\boldsymbol{q}, \nu) = \frac{g\, d_{\boldsymbol{k}} d_{\boldsymbol{k}'}}{(\xi_0/\xi)^2 + \xi_0^2 |\boldsymbol{q}|^2 - i[\nu/(c(\hat{\boldsymbol{q}})|\boldsymbol{q}|)]}\ , \tag{3·16}$$

where $\boldsymbol{q}$ and ν is the momentum and energy transfer, respectively. The parameters g, ξ_0 and $c(\hat{\boldsymbol{q}})$ can be treated as constants, whereas the correlation length ξ depends sensitively on control parameters and temperature. The behavior of $\xi(\delta, T)$ in the critical region is strongly influenced by interactions of order parameter fluctuations.

§4. Single-particle excitations

In this section, we analyze the low energy behavior of single-particle excitations in the presence of critical d-wave Fermi surface fluctuations.[15),16)] All fluctuation effects are encoded in the self-energy. We compute the self-energy explicitly within the random phase approximation, that is, to first order in the singular interaction $\Gamma_{\boldsymbol{k}\boldsymbol{k}'}(\boldsymbol{q}, \nu)$, and then briefly discuss corrections due to higher order terms.

4.1. *Random phase approximation*

To first order in Γ, the self-energy is given by the Feynman diagram (Fock term) shown in Fig. 3. The Hartree term vanishes because the expectation value of the d-wave density operator vanishes in the symmetric phase. The analytic expression

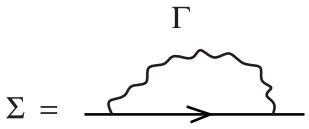

Fig. 3. Fock diagram relating the self-energy Σ to the dynamical effective interaction Γ.

corresponding to the Fock diagram reads

$$\Sigma(\boldsymbol{k}, i\omega_n) = -T \sum_{\nu_n} \int \frac{d^2q}{(2\pi)^2}\, \Gamma_{\boldsymbol{k}\boldsymbol{k}}(\boldsymbol{q}, i\nu_n)\, G(\boldsymbol{k}+\boldsymbol{q}, i\omega_n + i\nu_n)\, e^{i0^+(\omega_n+\nu_n)} \;, \qquad (4{\cdot}1)$$

where G is the propagator of the interacting system in a self-consistent perturbation expansion, which is replaced by the bare propagator G_0 in a non-selfconsistent calculation. We have approximated $\Gamma_{\boldsymbol{k}\boldsymbol{k}'}$ with $\boldsymbol{k}' = \boldsymbol{k}+\boldsymbol{q}$ by $\Gamma_{\boldsymbol{k}\boldsymbol{k}}$, which makes almost no difference since only small $\boldsymbol{q}$ contribute and the effective interaction does not vary rapidly as a function of $\boldsymbol{k}$ and $\boldsymbol{k}'$. The analytic continuation from imaginary to real frequencies yields

$$\begin{aligned}\Sigma(\boldsymbol{k}, \omega + i0^+) = -\frac{1}{\pi} \int d\nu \int \frac{d^2q}{(2\pi)^2} \big[& b(\nu)\, \mathrm{Im}\Gamma_{\boldsymbol{k}\boldsymbol{k}}(\boldsymbol{q}, \nu + i0^+)\, G(\boldsymbol{k}+\boldsymbol{q}, \nu+\omega+i0^+) \\ & - f(\nu)\, \Gamma_{\boldsymbol{k}\boldsymbol{k}}(\boldsymbol{q}, \nu-\omega-i0^+)\, \mathrm{Im}G(\boldsymbol{k}+\boldsymbol{q}, \nu+i0^+)\big] \;, \qquad (4{\cdot}2)\end{aligned}$$

where $b(\nu) = [e^{\beta\nu}-1]^{-1}$ is the Bose, and $f(\nu) = [e^{\beta\nu}+1]^{-1}$ the Fermi function. It is convenient to focus on the imaginary part of Σ, from which the real part can be easily obtained via the Kramers-Kronig relation. Using Eq. (3·6) to express the effective interaction by the dynamical Stoner factor, $\mathrm{Im}\Sigma$ can be expressed as

$$\mathrm{Im}\Sigma(\boldsymbol{k}, \omega) = -\frac{g\, d_{\boldsymbol{k}}^2}{\pi} \int d\nu \int \frac{d^2q}{(2\pi)^2} \big[b(\nu) + f(\nu+\omega)\big]\, \mathrm{Im}S_d(\boldsymbol{q}, \nu)\, \mathrm{Im}G(\boldsymbol{k}+\boldsymbol{q}, \omega+\nu) \;. \qquad (4{\cdot}3)$$

Here and in the following G, Σ, and S_d are retarded functions, that is, the real frequency axis is approached from above. The imaginary part of S_d can be written as

$$\mathrm{Im}S_d(\boldsymbol{q}, \nu) = \frac{c(\hat{\boldsymbol{q}})\, |\boldsymbol{q}|\, \nu}{\nu^2 + [(\xi_0/\xi)^2 + (\xi_0|\boldsymbol{q}|)^2]^2\, [c(\hat{\boldsymbol{q}})\, |\boldsymbol{q}|]^2} \;. \qquad (4{\cdot}4)$$

In the non-selfconsistent calculation one can exploit the relation $\mathrm{Im}G_0(\boldsymbol{p}, \omega) = -\pi\delta(\omega - \xi_{\boldsymbol{p}})$, where $\xi_{\boldsymbol{p}} = \epsilon_{\boldsymbol{p}} - \mu$, to perform the ν-integral analytically, which yields

$$\mathrm{Im}\Sigma(\boldsymbol{k}, \omega) = g\, d_{\boldsymbol{k}}^2 \int \frac{d^2q}{(2\pi)^2} \big[b(\xi_{\boldsymbol{k}+\boldsymbol{q}} - \omega) + f(\xi_{\boldsymbol{k}+\boldsymbol{q}})\big]\, \mathrm{Im}S_d(\boldsymbol{q}, \xi_{\boldsymbol{k}+\boldsymbol{q}} - \omega) \;. \qquad (4{\cdot}5)$$

We are interested in the renormalization of *low energy* excitations, with $\boldsymbol{k}$ close to the Fermi surface. Furthermore, only small momentum transfers $\boldsymbol{q}$ contribute to the self-energy. It is therefore convenient to introduce a local coordinate system in momentum space, centered around the Fermi point $\boldsymbol{k}_F$ which is reached from $\boldsymbol{k}$ by a projection on the Fermi surface (see Fig. 4), such that the vector $\boldsymbol{k}-\boldsymbol{k}_F$ is

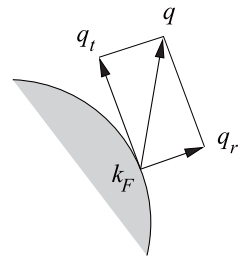

Fig. 4. Decomposition of momentum transfers $\boldsymbol{q}$ in radial and tangential components relative to the Fermi surface in $\boldsymbol{k}_F$.

perpendicular to the Fermi surface in $\boldsymbol{k}_F$. We can then parametrize $\boldsymbol{k}$ by the variable $k_r = \pm|\boldsymbol{k}–\boldsymbol{k}_F|$, with a positive sign for $\boldsymbol{k}$ on the exterior side of the Fermi surface, and minus inside. The momentum transfer $\boldsymbol{q}$ can be parametrized by a radial variable q_r and a tangential variable q_t, as shown in Fig. 4.

The energy variable $\xi_{\boldsymbol{k}+\boldsymbol{q}}$ appearing in the above expressions for $\mathrm{Im}\Sigma$ can be expanded as $\xi_{\boldsymbol{k}+\boldsymbol{q}} = v_{\boldsymbol{k}_F} k_r + v_{\boldsymbol{k}_F} q_r + \frac{1}{2m^t_{\boldsymbol{k}_F}}\, q_t^2$ for small $\boldsymbol{q}$ and $\boldsymbol{k}$ near $\boldsymbol{k}_F$. The parameter $m^t_{\boldsymbol{k}_F}$ is given by the second derivative of $\xi_{\boldsymbol{k}}$ in tangential direction, $(m^t_{\boldsymbol{k}_F})^{-1} = \partial^2_{k_t} \xi_{\boldsymbol{k}}|_{\boldsymbol{k}=\boldsymbol{k}_F}$. The term of order q_t^2 has been included since some asymptotic results are dominated by contributions with $|q_t| \gg |q_r|$. It is convenient to use $q_r' = q_r + \frac{1}{2m^t_{\boldsymbol{k}_F} v_{\boldsymbol{k}_F}}\, q_t^2$ instead of q_r as integration variable (in addition to q_t), since the excitation energy $\xi_{\boldsymbol{k}+\boldsymbol{q}} = v_{\boldsymbol{k}_F}(k_r + q_r')$ is linear in that variable. The Jacobi determinant corresponding to this change of variables is one.

4.2. *Ground state*

At $T = 0$, the combination of Bose and Fermi functions contributing to $\mathrm{Im}\Sigma(\boldsymbol{k}, \omega)$ reduces to a step function. In the following we restrict to the case $\omega > 0$ in derivations, but state final results also for $\omega < 0$.

At the quantum critical point ($T = 0$, $\xi = \infty$), the self-energy Eq. (4·5) can be written as

$$\mathrm{Im}\Sigma(\boldsymbol{k}, \omega) = g\, d^2_{\boldsymbol{k}_F} \int_{-k_r}^{\frac{\omega}{v_{\boldsymbol{k}_F}} - k_r} \frac{dq_r'}{2\pi} \int \frac{dq_t}{2\pi}\, \frac{c(\hat{\boldsymbol{q}})\, |\boldsymbol{q}|\, [\omega - v_{\boldsymbol{k}_F}(k_r + q_r')]}{[\omega - v_{\boldsymbol{k}_F}(k_r + q_r')]^2 + \xi_0^4\, [c(\hat{\boldsymbol{q}})]^2\, |\boldsymbol{q}|^6} \qquad (4{\cdot}6)$$

for $\omega > 0$. Imposing a cutoff on the q_t-integral would not affect the asymptotic behavior for small ω.

For $\boldsymbol{k} = \boldsymbol{k}_F$, that is for $k_r = 0$, the asymptotic ω-dependence of $\mathrm{Im}\Sigma$ can be extracted by using dimensionless variables $\tilde{q}_r$ and $\tilde{q}_t$ defined by $q_r' = (\omega / v_{\boldsymbol{k}_F})\, \tilde{q}_r$ and $q_t = (\xi_0^2\, c_{\boldsymbol{k}_F})^{-1/3} \omega^{1/3} \tilde{q}_t$, respectively. Here $c_{\boldsymbol{k}_F} = c(\boldsymbol{t}_{\boldsymbol{k}_F})$, where $\boldsymbol{t}_{\boldsymbol{k}_F}$ is a unit vector tangential to the Fermi surface in $\boldsymbol{k}_F$. For small ω and $k_r = 0$ the above $\boldsymbol{q}$-integral is dominated by almost tangential $\boldsymbol{q}$-vectors, that is $|q_t| \gg |q_r|$; more precisely $|q_r'|$ scales as $|q_t|^3$, and $|q_r|$ consequently as $|q_t|^2$. We can thus replace $|\boldsymbol{q}|$ by $|q_t|$ and $c(\hat{\boldsymbol{q}})$

by $c_{\boldsymbol{k}_F}$. This yields, for $\omega \to 0$,

$$\mathrm{Im}\Sigma(\boldsymbol{k}_F,\omega) = \frac{g\, d^2_{\boldsymbol{k}_F}}{v_{\boldsymbol{k}_F}} \frac{c^{1/3}_{\boldsymbol{k}_F}\,\omega^{2/3}}{\xi_0^{4/3}} \int_0^1 \frac{d\tilde{q}_r}{2\pi} \int_{-\infty}^{\infty} \frac{d\tilde{q}_t}{2\pi} \frac{|\tilde{q}_t|\,(1-\tilde{q}_r)}{(1-\tilde{q}_r)^2+\tilde{q}_t^6}\ . \tag{4·7}$$

This asymptotic result does not depend on any cutoff. The integral can be done analytically and yields the number $(4\sqrt{3}\pi)^{-1}$. For $\omega < 0$ one obtains the same expression with $(-\omega)^{2/3}$. We have thus shown that

$$\mathrm{Im}\Sigma(\boldsymbol{k}_F,\omega) = \frac{g\, d^2_{\boldsymbol{k}_F}}{4\sqrt{3}\pi\, v_{\boldsymbol{k}_F}} \frac{c^{1/3}_{\boldsymbol{k}_F}}{\xi_0^{4/3}}\, |\omega|^{2/3} \tag{4·8}$$

for small $|\omega|$. Note that $\nu = v_{\boldsymbol{k}_F} q_r' - \omega = (\tilde{q}_r - 1)\,\omega$ vanishes faster than $|\boldsymbol{q}|$ for $\omega \to 0$, which justifies our expansion of $S_d(\boldsymbol{q},\nu)$ for small ratios $\nu/|\boldsymbol{q}|$.

Not surprisingly, $\mathrm{Im}\Sigma(\boldsymbol{k}_F,\omega)$ has the same energy dependence as for the quantum critical points near phase separation[27] and ferromagnetism[28] in two dimensions, and also for fermions coupled to a $U(1)$-gauge field.[29),30] What differs, however, is the d-wave form factor making $\mathrm{Im}\Sigma(\boldsymbol{k}_F,\omega)$ strongly anisotropic. It is strongest near the van Hove points, while the leading terms vanish on the Brillouin zone diagonal.

A strongly anisotropic decay rate for single-particle excitations obeying a power-law with exponent 2/3 has also been found for an isotropic continuum (instead of lattice) version of our model.[14] However, that result was obtained for the symmetry-broken "nematic" phase, and the large anisotropic decay rate is due to the anisotropy of the nematic state and its Goldstone modes. At the quantum critical point the decay rate for the isotropic model also obeys a power law with exponent 2/3, but isotropically over the whole Fermi surface.[14]

For $\boldsymbol{k} \neq \boldsymbol{k}_F$, that is, for finite k_r, the asymptotic behavior of $\mathrm{Im}\Sigma(\boldsymbol{k},\omega)$, Eq. (4·6), is found by rewriting the integral with a dimensionless variable $\tilde{q}_r$ defined by $q_r' + k_r = (\omega/v_{\boldsymbol{k}_F})\,\tilde{q}_r$, and $\tilde{q}_t$ defined by $q_t = (\xi_0^2 c)^{-1/3}\omega^{1/3}\tilde{q}_t$. Here we approximate the velocity $c(\hat{\boldsymbol{q}})$ by a constant c. In the limit $\omega \to 0$ one can replace $|\boldsymbol{q}|$ by $\sqrt{q_t^2+k_r^2}$. Carrying out the $\tilde{q}_r$-integral one then obtains

$$\mathrm{Im}\Sigma(\boldsymbol{k},\omega) = \frac{g\, d^2_{\boldsymbol{k}_F}}{2\pi\, v_{\boldsymbol{k}_F}} \frac{c^{1/3}\,|\omega|^{2/3}}{\xi_0^{4/3}} \int_0^{\infty} \frac{d\tilde{q}_t}{2\pi} \sqrt{\tilde{q}_t^2+\kappa^2}\, \ln\left[1+\frac{1}{(\tilde{q}_t^2+\kappa^2)^3}\right]\ , \tag{4·9}$$

with $\kappa = (c\xi_0^2/|\omega|)^{1/3}\, k_r$. Two different asymptotic regimes are separated by the frequency scale

$$\omega_{k_r} = c\xi_0^2\,|k_r|^3\ . \tag{4·10}$$

For $|\omega| \gg \omega_{k_r}$, corresponding to $\kappa \ll 1$, one recovers the previous result Eq. (4·8), while for $|\omega| \ll \omega_{k_r}$ one can expand the integrand in κ^{-1} to obtain

$$\mathrm{Im}\Sigma(\boldsymbol{k},\omega) = \frac{g\, d^2_{\boldsymbol{k}_F}}{6\pi^2\, v_{\boldsymbol{k}_F}} \frac{1}{c\,\xi_0^4\, k_r^4}\,\omega^2\ . \tag{4·11}$$

In the latter limit momentum transfers normal to the Fermi surface dominate, and the above result can thus be easily generalized to a direction dependent $c(\hat{\boldsymbol{q}})$ replacing c by $c(\boldsymbol{n}_{\boldsymbol{k}_F})$. Note that for small k_r the low frequency behavior of $\mathrm{Im}\Sigma(\boldsymbol{k},\omega)$ deviates from $|\omega|^{2/3}$-behavior only below a tiny scale of order $|k_r|^3$. The same crossover has been obtained previously for fermions coupled to a $U(1)$ gauge field.[30)]

We now investigate the behavior of $\mathrm{Im}\Sigma(\boldsymbol{k}_F,\omega)$ at $T=0$ in the symmetric phase at a small distance from the quantum critical point, where the correlation length ξ is large, but not infinite. Using the same dimensionless variables $\tilde{q}_r$ and $\tilde{q}_t$ as for $\xi=\infty$, one finds that the $\boldsymbol{q}$-integral is still dominated by tangential momentum transfers for small ω, such that we can approximate $|\boldsymbol{q}|$ by $|q_t|$ and $c(\hat{\boldsymbol{q}})$ by $c_{\boldsymbol{k}_F}$. The $\tilde{q}_r$-integral can then be performed analytically, yielding

$$\mathrm{Im}\Sigma(\boldsymbol{k}_F,\omega) = \frac{g\, d_{\boldsymbol{k}_F}^2}{2\pi\, v_{\boldsymbol{k}_F}} \frac{c_{\boldsymbol{k}_F}^{1/3}\,|\omega|^{2/3}}{\xi_0^{4/3}} \int_0^\infty \frac{d\tilde{q}_t}{2\pi}\, \tilde{q}_t\, \ln\left[1+\frac{1}{\tilde{q}_t^2(\tilde{q}_t^2+\zeta^2)^2}\right] , \tag{4·12}$$

with $\zeta = (c_{\boldsymbol{k}_F}\xi_0^2/|\omega|)^{1/3}\xi^{-1}$. There are two asymptotic regimes, separated by the characteristic frequency scale

$$\omega_\xi = c_{\boldsymbol{k}_F}\xi_0^2/\xi^3 = c_{\boldsymbol{k}_F}\xi_0^{-1}S_d^{-3/2} . \tag{4·13}$$

For $|\omega| \gg \omega_\xi$ one has $\zeta \ll 1$, and one recovers the previous result Eq. (4·8). For $|\omega| \ll \omega_\xi$, an expansion of the integral yields the asymptotic behavior

$$\mathrm{Im}\Sigma(\boldsymbol{k}_F,\omega) = \frac{g\, d_{\boldsymbol{k}_F}^2}{6\pi^2\, v_{\boldsymbol{k}_F}} \frac{\xi^4}{c_{\boldsymbol{k}_F}\xi_0^4}\,\omega^2\, \ln\frac{\omega_\xi}{|\omega|} . \tag{4·14}$$

Hence, below the scale ω_ξ one obtains Fermi liquid behavior. Close to the quantum critical point, that is for large ξ and S_d, the crossover from $|\omega|^{2/3}$ scaling to Fermi liquid behavior sets in only for tiny frequencies, and the coefficient in front of the asymptotic $\omega^2 \log \frac{\omega_\xi}{|\omega|}$ law is anomalously large.

4.3. *Low finite temperature*

At $T>0$ the non-selfconsistent RPA self-energy, Eq. (4·5), has the form

$$\mathrm{Im}\Sigma(\boldsymbol{k},\omega) = g\, d_{\boldsymbol{k}_F}^2 \int \frac{dq_r'}{2\pi} \int \frac{dq_t}{2\pi} \left\{ b[v_{\boldsymbol{k}_F}(k_r+q_r')-\omega] + f[v_{\boldsymbol{k}_F}(k_r+q_r')] \right\}$$
$$\times \frac{c(\hat{\boldsymbol{q}})\,|\boldsymbol{q}|\,[v_{\boldsymbol{k}_F}(k_r+q_r')-\omega]}{[v_{\boldsymbol{k}_F}(k_r+q_r')-\omega]^2 + [(\xi_0/\xi)^2+(\xi_0\,|\boldsymbol{q}|)^2]^2\,[c(\hat{\boldsymbol{q}})\,|\boldsymbol{q}|]^2} . \tag{4·15}$$

To extract the asymptotic behavior of this integral for low T, small ω and small k_r, it is helpful to consider first the special case $k_r=\omega=0$, that is

$$\mathrm{Im}\Sigma(\boldsymbol{k}_F,0) = g\, d_{\boldsymbol{k}_F}^2 \int \frac{dq_r'}{2\pi} \int \frac{dq_t}{2\pi} \left[b(v_{\boldsymbol{k}_F}q_r') + f(v_{\boldsymbol{k}_F}q_r') \right]$$
$$\times \frac{c(\hat{\boldsymbol{q}})\,|\boldsymbol{q}|\,v_{\boldsymbol{k}_F}q_r'}{(v_{\boldsymbol{k}_F}q_r')^2 + [(\xi_0/\xi)^2+(\xi_0\,|\boldsymbol{q}|)^2]^2\,[c(\hat{\boldsymbol{q}})\,|\boldsymbol{q}|]^2} . \tag{4·16}$$

We introduce dimensionless variables $\tilde{q}_r$ and $\tilde{q}_t$ defined by the relations $q_r' = \xi_0^2\,\tilde{q}_r/\xi^3$ and $q_t = \tilde{q}_t/\xi$, respectively. We assume that ξ diverges faster than $T^{-1/3}$ for $T \to 0$, as is indeed the case when we approach the quantum critical point from the quantum critical region.[25] Then the above integral is dominated by momenta with a small ratio $v_{\boldsymbol{k}_F} q_r'/T$, such that the Bose function can be expanded as $b(v_{\boldsymbol{k}_F} q_r') \to T/(v_{\boldsymbol{k}_F} q_r')$, and the Fermi function can be neglected. Furthermore we can take advantage of the fact that the integral is dominated by momenta $\boldsymbol{q}$ which are almost tangential to the Fermi surface for large ξ, since $|q_r'|$ scales as $|q_t|^3$, and hence $|q_r|$ as $|q_t|^2$. We can thus substitute $|\boldsymbol{q}|$ by $|q_t|$ and $c(\hat{\boldsymbol{q}})$ by $c_{\boldsymbol{k}_F}$, and find the simple result

$$\begin{aligned} \mathrm{Im}\Sigma(\boldsymbol{k}_F, 0) &\to \frac{g\, d_{\boldsymbol{k}_F}^2}{\xi_0^2}\, T\, \xi \int_{-\infty}^{\infty} \frac{d\tilde{q}_r}{2\pi} \int_{-\infty}^{\infty} \frac{d\tilde{q}_t}{2\pi}\, \frac{c_{\boldsymbol{k}_F}\, |\tilde{q}_t|}{(v_{\boldsymbol{k}_F}\tilde{q}_r)^2 + (1+\tilde{q}_t^2)^2\, (c_{\boldsymbol{k}_F}\tilde{q}_t)^2} \\ &= \frac{g\, d_{\boldsymbol{k}_F}^2}{4 v_{\boldsymbol{k}_F} \xi_0^2}\, T\, \xi \end{aligned} \tag{4·17}$$

for $T \to 0$. A similar contribution of order $T\xi$ has been found previously for almost antiferromagnetic[31),32)] and almost ferromagnetic[33)] metals. Note that the $T^{2/3}$-law proposed for $\mathrm{Im}\Sigma(\boldsymbol{k}_F, 0)$ in Ref. 15), which one might expect by identifying T and ω scaling, does not describe the leading asymptotic behavior at low T.

We now consider the case of finite frequencies ω, which shall however be sufficiently small that we can still use the expansion of the Bose function and neglect the Fermi function. We set $\omega = v_{\boldsymbol{k}_F} x/\xi$, where x is a dimensionless scaling variable which is kept fixed in the low temperature limit. Once again we use dimensionless integration variables $\tilde{q}_r$ and $\tilde{q}_t$, now defined by $q_r' - \omega/v_{\boldsymbol{k}_F} = \xi_0^2\,\tilde{q}_r/\xi^3$ and $q_t = \tilde{q}_t/\xi$, respectively. For $\xi \to \infty$ we can then replace q_r in $|\boldsymbol{q}| = \sqrt{q_t^2 + q_r^2}$ by $\omega/v_{\boldsymbol{k}_F}$, which yields $|\boldsymbol{q}| = \tilde{q}/\xi$ with $\tilde{q} = \sqrt{\tilde{q}_t^2 + x^2}$. The Bose function can again be expanded and the Fermi function neglected for $T \to 0$, for ξ diverging faster than $T^{-1/3}$, and we obtain

$$\mathrm{Im}\Sigma(\boldsymbol{k}_F, \omega) \to \frac{g\, d_{\boldsymbol{k}_F}^2}{4 v_{\boldsymbol{k}_F} \xi_0^2}\, T\, \xi\, l(x) \tag{4·18}$$

with a dimensionless scaling function

$$l(x) = \int_{-\infty}^{\infty} \frac{d\tilde{q}_r}{2\pi} \int_{-\infty}^{\infty} \frac{d\tilde{q}_t}{2\pi}\, \frac{4\, v_{\boldsymbol{k}_F}\, c(\hat{\boldsymbol{q}})\, \tilde{q}}{(v_{\boldsymbol{k}_F}\tilde{q}_r)^2 + (1+\tilde{q}^2)^2\, [c(\hat{\boldsymbol{q}})\, \tilde{q}]^2}. \tag{4·19}$$

The unit vector $\hat{\boldsymbol{q}}$ can be parametrized by x and $\tilde{q}_t$, it does not depend on $\tilde{q}_r$. Performing the elementary $\tilde{q}_r$-integral, the velocities $v_{\boldsymbol{k}_F}$ and $c(\hat{\boldsymbol{q}})$ in the above expression for $l(x)$ drop out completely. Carrying out the remaining $\tilde{q}_t$-integral, we find the simple universal result

$$l(x) = \frac{1}{\sqrt{1+x^2}}\,. \tag{4·20}$$

For $\omega = 0$ the previous result for $\mathrm{Im}\Sigma(\boldsymbol{k}_F, 0)$ is recovered. For large x the scaling function decays as x^{-1}. Hence, the contribution from the Bose function singularity to $\mathrm{Im}\Sigma(\boldsymbol{k}_F, \omega)$ leads to a peak with an amplitude scaling as $T\xi(T)$ and a width of

order $v_{\boldsymbol{k}_F}/\xi(T)$. The product of amplitude and width is thus proportional to T. Since the contribution proportional to the Bose function to $\mathrm{Im}\Sigma(\boldsymbol{k},\omega)$, Eq. (4·15), depends only via the linear combination $\omega - v_{\boldsymbol{k}_F} k_r$ on ω and k_r, the right-hand side of Eq. (4·18) is applicable also for $\boldsymbol{k} \neq \boldsymbol{k}_F$, where it yields the contribution from the expanded Bose term for $T \to 0,\ \omega \to v_{\boldsymbol{k}_F} k_r$, with fixed $x = (\omega/v_{\boldsymbol{k}_F} - k_r)\,\xi$.

The asymptotic behavior derived above is entirely due to *"classical"* fluctuations, corresponding to the contribution with $\nu_n = 0$ to the Matsubara frequency sum in Eq. (4·1). The analytic continuation of that contribution to real frequencies reads

$$\Sigma^c(\boldsymbol{k},\omega) = -T \int \frac{d^2q}{(2\pi)^2}\, \Gamma_{\boldsymbol{k}\boldsymbol{k}}(\boldsymbol{q},0)\, G(\boldsymbol{k}+\boldsymbol{q},\omega). \tag{4·21}$$

Note that $\Gamma_{\boldsymbol{k}\boldsymbol{k}}(\boldsymbol{q},0)$ is real and does not depend on the parameter $c(\hat{\boldsymbol{q}})$. For $G = G_0$ one can easily show that indeed

$$\mathrm{Im}\Sigma^c(\boldsymbol{k},\omega) \to \frac{g\, d_{\boldsymbol{k}_F}^2}{4 v_{\boldsymbol{k}_F} \xi_0^2}\, T\, \xi\, l[(\omega/v_{\boldsymbol{k}_F} - k_r)\xi] \tag{4·22}$$

with $l(x)$ from Eq. (4·20).

We now split the total self-energy in two parts, $\Sigma = \Sigma^c + \Sigma^q$, where the "quantum" contribution is obtained by summing Matsubara frequencies $\nu_n \neq 0$ in Eq. (4·1). After analytical continuation to real frequencies, $\mathrm{Im}\Sigma^c$ was obtained from the Bose function singularity T/ν. To analyze $\mathrm{Im}\Sigma^q$ for real frequencies we thus subtract T/ν from the Bose function, that is we replace $b(\nu)$ by the regular function $\bar{b}(\nu) = b(\nu) - T/\nu$ in Eq. (4·15). The asymptotic behavior of $\mathrm{Im}\Sigma^q$ at low frequency and low temperature can be extracted by using the same dimensionless variables $\tilde{q}_t$ and $\tilde{q}_r$ as already in the case $T = 0$, and scaling ω as T by keeping $\tilde{\omega} = \omega/T$ fixed in the limit $T \to 0$, $\omega \to 0$. Asymptotically one can replace $|\boldsymbol{q}|$ by $|q_t|$ and $c(\hat{\boldsymbol{q}})$ by $c_{\boldsymbol{k}_F}$ as for $T = 0$. Furthermore one can neglect ξ^{-2} in the denominator of $\mathrm{Im}S_d$ since ξ^{-2} scales to zero faster than $|\boldsymbol{q}|^2$. The $\tilde{q}_t$-integral can then be done analytically, and we obtain

$$\mathrm{Im}\Sigma^q(\boldsymbol{k}_F,\omega) \to \frac{g\, d_{\boldsymbol{k}_F}^2}{v_{\boldsymbol{k}_F}}\, \frac{c_{\boldsymbol{k}_F}^{1/3}\, |\omega|^{2/3}}{\xi_0^{4/3}}\, s(\tilde{\omega})\ , \tag{4·23}$$

with the dimensionless scaling function

$$s(\tilde{\omega}) = \frac{\mathrm{sgn}(\tilde{\omega})}{3\sqrt{3}} \int_{-\infty}^{\infty} \frac{d\tilde{q}_r}{2\pi} \left[\frac{1}{e^{\tilde{\omega}(\tilde{q}_r - 1)} - 1} - \frac{1}{\tilde{\omega}(\tilde{q}_r - 1)} + \frac{1}{e^{\tilde{\omega}\tilde{q}_r} + 1} \right] \frac{\tilde{q}_r - 1}{|1 - \tilde{q}_r|^{4/3}}\ . \tag{4·24}$$

For $|\tilde{\omega}| \to \infty$ the scaling function tends to $\frac{1}{4\sqrt{3}\pi}$, and one recovers the zero temperature result, Eq. (4·8). The convergence to the zero temperature limit is however rather slow. For small $|\tilde{\omega}|$, $s(\tilde{\omega})$ is negative and proportional to $|\tilde{\omega}|^{-2/3}$, such that

$$\mathrm{Im}\Sigma^q(\boldsymbol{k}_F,0) \to \alpha\, \frac{g\, d_{\boldsymbol{k}_F}^2}{v_{\boldsymbol{k}_F}}\, \frac{c_{\boldsymbol{k}_F}^{1/3}}{\xi_0^{4/3}}\, T^{2/3}\ , \tag{4·25}$$

where $\alpha \approx -0.15$ is a constant. We note that $\mathrm{Im}\Sigma^q(\boldsymbol{k}_F,0)$ is positive but smaller than the absolute value of the classical contribution for low T, since the latter is

proportional to $T\xi$, such that the imaginary part of $\Sigma^c + \Sigma^q$ remains negative, as required. For $\boldsymbol{k} \neq \boldsymbol{k}_F$, that is for finite k_r, the momentum dependence of $\mathrm{Im}\Sigma^q(\boldsymbol{k}, \omega)$ is negligible for $|\omega| \gg \omega_{k_r}$, with $\omega_{k_r} = c\xi_0^2 |k_r|^3$, as in the ground state.

In summary, at low finite T the RPA self-energy is given by a classical contribution Σ^c of order $T\xi$, and a quantum contribution Σ^q of order $T^{2/3}$ and $|\omega|^{2/3}$, which obeys ω/T-scaling. A similar structure of the self-energy, with a classical part and a quantum part obeying (ω/T)-scaling, has been obtained also for electrons coupled to strong ferromagnetic[33] or antiferromagnetic[32] fluctuations in the quantum critical regime.

4.4. *Self-consistency and vertex corrections*

The self-energy obtained above strongly modifies the propagator G, compared to the bare propagator G_0. Since Σ was computed from the Fock diagram with the bare propagator G_0, the question of self-consistency arises.

At $T = 0$, replacing G_0 by G in the Fock diagram does not change the result. The self-energy in the internal propagator drops out completely when the loop integral is done.[16] Hence, the above result for Σ is already the self-consistent one at zero temperature.

At $T > 0$, the quantum part of the self-energy, Σ^q, remains almost unaffected by self-consistency, but the classical part Σ^c changes more strongly. However, the leading temperature dependence at zero frequency in the quantum critical regime, $\mathrm{Im}\Sigma(k_F, \omega) \propto T\xi(T)$, remains the same.[16]

Vertex corrections to the Fock diagram seem to lead only to moderate finite renormalizations, leaving the qualitative behavior of the self-energy unchanged. At the quantum critical point, this can be deduced from the earlier analysis of vertex corrections in the analogous problem of fermions coupled to a $U(1)$ gauge field,[34] which was confirmed in a very careful recent work in the context of quantum criticality.[35] By virtue of ω/T scaling, one may expect that quantum contributions (from finite Matsubara frequencies) to vertex corrections behave similarly at zero and low finite temperatures, and lead to finite renormalizations only. By contrast, contributions from classical fluctuations at $T > 0$ have no counterpart at $T = 0$ and might thus behave differently. However, an explicit calculation of the classical first order vertex correction also yields a finite result.[16]

4.5. *Dispersion and decay of excitations*

The momentum resolved spectral function for single particle excitations is determined by the self-energy as

$$A(\boldsymbol{k}, \omega) = -\frac{1}{\pi} \mathrm{Im} \frac{1}{\omega - \xi_{\boldsymbol{k}} - \Sigma(\boldsymbol{k}, \omega)} \,. \tag{4·26}$$

At the quantum critical point the asymptotic low-energy result for the self-energy reads[16]

$$\Sigma(\boldsymbol{k}, \omega) \to \Sigma_{\boldsymbol{k}_F}(\omega) = -C_{\boldsymbol{k}_F} \left[\mathrm{sgn}(\omega) + \frac{i}{\sqrt{3}} \right] |\omega|^{2/3} \,, \tag{4·27}$$

where

$$C_{\boldsymbol{k}_F} = \frac{|g|\, d_{\boldsymbol{k}_F}^2}{4\pi\, v_{\boldsymbol{k}_F}} \frac{c_{\boldsymbol{k}_F}^{1/3}}{\xi_0^{4/3}} \,. \tag{4·28}$$

The real part of Σ is simply the Kramers-Kronig transform of the imaginary part. Strictly speaking, this simple k_r-independent behavior is valid only for $|\omega| \gg \omega_{k_r}$, but the scale ω_{k_r} is proportional to k_r^3 and thus tiny for $\boldsymbol{k}$ near the Fermi surface. The prefactor $C_{\boldsymbol{k}_F}$ depends strongly on the position of $\boldsymbol{k}_F$. It decreases rapidly for $\boldsymbol{k}_F$ near the Brillouin zone diagonal, where $d_{\boldsymbol{k}_F}$ vanishes, while it is enhanced near the van Hove points, where $v_{\boldsymbol{k}_F}$ becomes small. The $\boldsymbol{k}_F$-dependence of $c_{\boldsymbol{k}_F}^{1/3}$ is comparatively weak. The competition between ω and the self-energy in the denominator of $A(\boldsymbol{k},\omega)$ leads to the characteristic energy scale

$$\omega_c = C_{\boldsymbol{k}_F}^3 \propto \frac{d_{\boldsymbol{k}_F}^6}{v_{\boldsymbol{k}_F}^3} \,, \tag{4·29}$$

which obviously varies very strongly along the Fermi surface.

For fixed $\boldsymbol{k}$ with $|\xi_{\boldsymbol{k}}| \gg \omega_c$ the spectral function $A(\boldsymbol{k},\omega)$ has almost Lorentzian shape as a function of ω, with a maximum near $\omega = \xi_{\boldsymbol{k}}$ and a width of order $C_{\boldsymbol{k}_F}|\xi_{\boldsymbol{k}}|^{2/3}$. The life-time broadening thus decreases more slowly than the excitation energy $\xi_{\boldsymbol{k}}$, as $\boldsymbol{k}$ approaches the Fermi surface, such that no well-defined quasiparticles exist. For $|\xi_{\boldsymbol{k}}| \approx \omega_c$ the maximum of $A(\boldsymbol{k},\omega)$ is shifted strongly away from $\xi_{\boldsymbol{k}}$ and the width is of order of the peak energy. For $|\xi_{\boldsymbol{k}}| \ll \omega_c$ one can neglect ω compared to $\mathrm{Re}\Sigma(\boldsymbol{k},\omega)$ in Eq. (4·26), and $A(\boldsymbol{k},\omega)$ is now peaked at $\omega = \bar{\xi}_{\boldsymbol{k}}$, with the renormalized dispersion

$$\bar{\xi}_{\boldsymbol{k}} = \mathrm{sgn}(\xi_{\boldsymbol{k}})\, (C_{\boldsymbol{k}_F}^{-1}|\xi_{\boldsymbol{k}}|)^{3/2} \propto k_r^{3/2} \,. \tag{4·30}$$

Extracting a dispersion relation from the momentum dependence of the peak position in $A(\boldsymbol{k},\omega)$, one thus obtains a flat band with a vanishing slope near the Fermi surface. The width of the peak centered around $\bar{\xi}_{\boldsymbol{k}}$ is of order $C_{\boldsymbol{k}_F}|\bar{\xi}_{\boldsymbol{k}}|^{2/3} = |\xi_{\boldsymbol{k}}|$ and thus linear in k_r.

Momentum scans of $A(\boldsymbol{k},\omega)$ perpendicular to the Fermi surface at fixed ω lead to Lorentzian peaks centered around $k_r = \frac{1}{v_{\boldsymbol{k}_F}}[\omega + C_{\boldsymbol{k}_F}\mathrm{sgn}(\omega)|\omega|^{2/3}]$. The integral

$$\int \frac{dk_r}{2\pi}\, A(\boldsymbol{k},\omega) = \frac{1}{2\pi\, v_{\boldsymbol{k}_F}} \tag{4·31}$$

does not depend on the self-energy. The $\boldsymbol{k}$-integrated density of states at the Fermi level remains therefore unrenormalized, that is, it is determined by the bare Fermi velocity.

The most important temperature effect is that $\mathrm{Im}\Sigma(\boldsymbol{k}_F,0)$ increases quickly from zero to sizable finite values upon increasing T. For small T near the quantum critical point we obtained

$$\mathrm{Im}\Sigma(\boldsymbol{k}_F,0) \to \frac{g\, d_{\boldsymbol{k}_F}^2}{4 v_{\boldsymbol{k}_F} \xi_0^2}\, T\, \xi \propto \frac{d_{\boldsymbol{k}_F}^2}{v_{\boldsymbol{k}_F}} \sqrt{\frac{T}{|\log T|}} \tag{4·32}$$

both in the non-selfconsistent and self-consistent calculation. This cuts off the divergence of $A(\boldsymbol{k}_F,\omega)$ for $\omega\to 0$ occurring at zero temperature and replaces it by a maximum of order $\sqrt{|\log T|/T}$. Note that $\mathrm{Im}\Sigma(\boldsymbol{k}_F,0)$ vanishes much slower with T than in conventional Fermi liquids, where one has T^2 (in 3D) or $T^2|\log T|$ (in 2D) behavior.

§5. DC resistivity

We now turn to the computation of the DC resistivity and the corresponding transport decay rate, which turns out to be much smaller than the decay rate of single-particle excitations.[17)]

The DC charge conductivity can be obtained from the retarded current-current correlator $\mathit{\Pi}_{jj'}(\boldsymbol{q},\omega)$ as

$$\sigma_{jj'} = -\lim_{\omega\to 0}\lim_{\boldsymbol{q}\to\boldsymbol{0}}\frac{e^2}{\omega}\,\mathrm{Im}\mathit{\Pi}_{jj'}(\boldsymbol{q},\omega)\;. \tag{5·1}$$

For electrons moving in a crystal with square lattice symmetry, the conductivity tensor is diagonal. The current-current correlator can be expressed in terms of the single-particle Green function G and current vertices, yielding

$$\sigma_{jj'} = -\frac{e^2}{\pi}\int d\omega\, f'(\omega)\int\frac{d^2k}{(2\pi)^2}\,\mathit{\Lambda}^0_j(\boldsymbol{k})\,|G(\boldsymbol{k},\omega)|^2\,\mathit{\Lambda}_{j'}(\boldsymbol{k},\omega)\;, \tag{5·2}$$

where $\boldsymbol{\mathit{\Lambda}}^0(\boldsymbol{k}) = \boldsymbol{v}_{\boldsymbol{k}} = \nabla\epsilon_{\boldsymbol{k}}$ is the bare current vertex, and $\boldsymbol{\mathit{\Lambda}}(\boldsymbol{k},\omega)$ is the interacting current vertex in the mixed advanced-retarded DC limit, that is, $\boldsymbol{\mathit{\Lambda}}(\boldsymbol{k},\omega) = \boldsymbol{\mathit{\Lambda}}(\boldsymbol{k},\omega+i0^+;\boldsymbol{k},\omega-i0^+)$. The product $|G|^2$ can be expressed in terms of the single-particle spectral function $A(\boldsymbol{k},\omega) = -\frac{1}{\pi}\mathrm{Im}G(\boldsymbol{k},\omega)$ and the (retarded) self-energy as $|G(\boldsymbol{k},\omega)|^2 = -\pi A(\boldsymbol{k},\omega)/\mathrm{Im}\Sigma(\boldsymbol{k},\omega)$. At low temperatures the derivative of the Fermi function $f'(\omega)$ has a sharp peak of width T at $\omega=0$. Since all other factors under the integral in Eq. (5·2) have a broader ω-dependence, one can replace $f'(\omega)$ by $-\delta(\omega)$, such that the conductivity can be written as

$$\sigma_{jj'} = -e^2\int\frac{d^2k}{(2\pi)^2}\,\mathit{\Lambda}^0_j(\boldsymbol{k})\,\frac{A(\boldsymbol{k},0)}{\mathrm{Im}\Sigma(\boldsymbol{k},0)}\mathit{\Lambda}_{j'}(\boldsymbol{k},0)\;. \tag{5·3}$$

The approximation for the current vertex corresponding to the RPA self-energy involves current vertex corrections given by the sum of all particle-hole ladder diagrams, in close analogy to the Born approximation for impurity scattering.[36)] We assume that the Pomeranchuk fluctuations thermalize sufficiently rapidly such that the effective interaction Eq. (3·16) is not modified by the electric current. This relaxation to equilibrium is not described by our model Eq. (2·1) and has to be provided by an additional mechanism such as impurity, umklapp or phonon scattering.[37),38)]

Summing all particle-hole ladders, and performing an analytic continuation to the real frequency axis, leads to the following linear integral equation for the current vertex

$$\boldsymbol{\mathit{\Lambda}}(\boldsymbol{k},\omega) = \boldsymbol{\mathit{\Lambda}}^0(\boldsymbol{k}) + \int d\epsilon\int\frac{d^2q}{(2\pi)^2}\,[b(\epsilon)+f(\omega+\epsilon)]$$

$$\times \, \mathrm{Im}\Gamma_{\boldsymbol{kk}}(\boldsymbol{q},\epsilon)\,\frac{A(\boldsymbol{k}+\boldsymbol{q},\omega+\epsilon)}{\mathrm{Im}\Sigma(\boldsymbol{k}+\boldsymbol{q},\omega+\epsilon)}\,\boldsymbol{\Lambda}(\boldsymbol{k}+\boldsymbol{q},\omega+\epsilon)\;. \tag{5·4}$$

Approaching the quantum critical point for $T \to 0$, the correlation length $\xi(T)$ diverges. Repeating the arguments used for the calculation of $\Sigma(\boldsymbol{k},\omega)$ in the preceding section, one finds that the integration variable ϵ in Eq. (5·4) scales as ξ^{-3} and can therefore be set to zero in the arguments of A, Σ, and $\boldsymbol{\Lambda}$ on the right-hand side of Eq. (5·4). Expanding the Bose function as $b(\epsilon) \sim T/\epsilon$, one can easily perform the ϵ-integration, $\int d\epsilon\,\epsilon^{-1}\,\mathrm{Im}\Gamma_{\boldsymbol{kk}}(\boldsymbol{q},\epsilon) = \pi\Gamma_{\boldsymbol{kk}}(\boldsymbol{q},0)$, yielding a closed equation for the *static* current vertex $\boldsymbol{\Lambda}(\boldsymbol{k}) = \boldsymbol{\Lambda}(\boldsymbol{k},0)$

$$\boldsymbol{\Lambda}(\boldsymbol{k}) = \boldsymbol{\Lambda}^0(\boldsymbol{k}) + T\int \frac{d^2q}{(2\pi)^2}\Gamma_{\boldsymbol{kk}}(\boldsymbol{q},0)\,\frac{\pi A(\boldsymbol{k}+\boldsymbol{q},0)}{\mathrm{Im}\Sigma(\boldsymbol{k}+\boldsymbol{q},0)}\,\boldsymbol{\Lambda}(\boldsymbol{k}+\boldsymbol{q})\;. \tag{5·5}$$

This result could have been obtained more directly by taking only the *classical* fluctuations into account, that is, by including only the term $\Gamma_{\boldsymbol{kk}}(\boldsymbol{q}, i\epsilon_n)$ with Matsubara frequency $\epsilon_n = 0$ in the Matsubara sums for the current vertex corrections.

Inserting the ansatz $\boldsymbol{\Lambda}(\boldsymbol{k}) = \lambda(\boldsymbol{k})\boldsymbol{v}_{\boldsymbol{k}}$ into the above equation, one obtains the following equation for $\lambda(\boldsymbol{k})$:

$$\boldsymbol{\lambda}(\boldsymbol{k}) = 1 + T\int \frac{d^2q}{(2\pi)^2}\Gamma_{\boldsymbol{kk}}(\boldsymbol{q},0)\,\frac{\pi A(\boldsymbol{k}+\boldsymbol{q},0)}{\mathrm{Im}\Sigma(\boldsymbol{k}+\boldsymbol{q},0)}\,\frac{\boldsymbol{v}_{\boldsymbol{k}}\cdot\boldsymbol{v}_{\boldsymbol{k}+\boldsymbol{q}}}{v_{\boldsymbol{k}}^2}\,\boldsymbol{\lambda}(\boldsymbol{k}+\boldsymbol{q})\;. \tag{5·6}$$

Since the conductivity is determined by momenta near the Fermi surface, we focus on the case $\boldsymbol{k} = \boldsymbol{k}_F$. For large ξ the above integral is dominated by small momentum transfers $\boldsymbol{q}$ of order ξ^{-1}, due to the effective interaction $\Gamma_{\boldsymbol{kk}}(\boldsymbol{q},0)$. The spectral function is peaked for momenta on the Fermi surface, with a width determined by $\mathrm{Im}\Sigma(\boldsymbol{k}_F,0)$, which is proportional to $T\xi(T)$. The self-energy $\Sigma(\boldsymbol{k},0)$ varies on a momentum scale of order ξ^{-1} for momentum shifts perpendicular to the Fermi surface. The same can be expected for $\lambda(\boldsymbol{k})$, since the current vertex correction can be related to the shift of the self-energy in the presence of a field coupled to the current operator. Since $T\xi^2(T) \propto 1/\log T$ in the quantum critical regime, and since the tangential $\boldsymbol{q}$-dependence of $\mathrm{Im}\Sigma(\boldsymbol{k}_F+\boldsymbol{q})$ and $\lambda(\boldsymbol{k}_F+\boldsymbol{q})$ is negligible on the scale ξ^{-1}, we can neglect the $\boldsymbol{q}$-dependence of $\mathrm{Im}\Sigma(\boldsymbol{k}_F+\boldsymbol{q})$ and $\lambda(\boldsymbol{k}_F+\boldsymbol{q})$ in Eq. (5·6), which can then be solved explicitly. The solution reads

$$\boldsymbol{\lambda}(\boldsymbol{k}_F) = \left[1 - \frac{\pi T}{\mathrm{Im}\Sigma(\boldsymbol{k}_F,0)}\int \frac{d^2q}{(2\pi)^2}\,\Gamma_{\boldsymbol{k}_F\boldsymbol{k}_F}(\boldsymbol{q},0)\,A(\boldsymbol{k}_F+\boldsymbol{q},0)\,\frac{\boldsymbol{v}_{\boldsymbol{k}_F}\cdot\boldsymbol{v}_{\boldsymbol{k}_F+\boldsymbol{q}}}{v_{\boldsymbol{k}_F}^2}\right]^{-1}\;. \tag{5·7}$$

Using

$$\mathrm{Im}\Sigma(\boldsymbol{k}_F,0) = \pi T\int \frac{d^2q}{(2\pi)^2}\,\Gamma_{\boldsymbol{k}_F\boldsymbol{k}_F}(\boldsymbol{q},0)\,A(\boldsymbol{k}_F+\boldsymbol{q},0)\;, \tag{5·8}$$

which is valid within self-consistent RPA restricted to classical fluctuations, one can write $\lambda_{\boldsymbol{k}_F}$ as

$$\lambda(\boldsymbol{k}_F) = \gamma_{\boldsymbol{k}_F}/\gamma^{\mathrm{tr}}_{\boldsymbol{k}_F}\;, \tag{5·9}$$

where $\gamma_{\boldsymbol{k}_F} = -\mathrm{Im}\Sigma(\boldsymbol{k}_F, 0)$ is the single-particle decay rate while

$$\gamma^{\mathrm{tr}}_{\boldsymbol{k}_F} = -\pi T \int \frac{d^2q}{(2\pi)^2}\, \Gamma_{\boldsymbol{k}_F \boldsymbol{k}_F}(\boldsymbol{q}, 0)\, A(\boldsymbol{k}_F + \boldsymbol{q}, 0) \left(1 - \frac{\boldsymbol{v}_{\boldsymbol{k}_F} \cdot \boldsymbol{v}_{\boldsymbol{k}_F + \boldsymbol{q}}}{v^2_{\boldsymbol{k}_F}}\right) . \tag{5·10}$$

is the scattering rate determining transport properties.

The momentum integral in the formula (5·3) for the conductivity is peaked at the Fermi surface. For $T \to 0$ with $\xi(T) \propto (T \log T)^{-1/2}$ one can substitute $A(\boldsymbol{k}, 0)$ under the integral by $\delta(\epsilon_{\boldsymbol{k}} - \mu)$, neglecting possible corrections of order $1/\log T$, such that the conductivity can be expressed as a Fermi surface integral. Inserting Eq. (5·9) for $\lambda(\boldsymbol{k}_F)$, one obtains

$$\sigma = \frac{e^2}{8\pi^2} \int d\Omega_{\boldsymbol{k}_F} \frac{v_{\boldsymbol{k}_F}}{\gamma^{\mathrm{tr}}_{\boldsymbol{k}_F}} \tag{5·11}$$

for the diagonal part $\sigma = \sigma_{jj}$ of the conductivity tensor.

To calculate $\gamma^{\mathrm{tr}}_{\boldsymbol{k}_F}$, we parametrize the small momentum transfer $\boldsymbol{q}$ in Eq. (5·10) by their radial and tangential components, q_r and q_t, respectively (see Fig. 4). For $T \to 0$, we can again approximate $A(\boldsymbol{k}_F + \boldsymbol{q}, 0)$ by a δ-function, $\delta(\epsilon_{\boldsymbol{k}_F + \boldsymbol{q}} - \mu)$. For the dispersion relation we use the expansion $\epsilon_{\boldsymbol{k}_F + \boldsymbol{q}} - \mu = v_{\boldsymbol{k}_F} q_r + q_t^2/(2m^t_{\boldsymbol{k}_F})$. Since $\boldsymbol{k}_F + \boldsymbol{q}$ is confined to the Fermi surface, the momentum transfers $\boldsymbol{q}$ are almost tangential to the Fermi surface in $\boldsymbol{k}_F$, such that the term of order q_t^2 cannot be neglected compared to the term linear in q_r. Expanding also the kinematic factor $1 - \frac{\boldsymbol{v}_{\boldsymbol{k}_F} \cdot \boldsymbol{v}_{\boldsymbol{k}_F + \boldsymbol{q}}}{v_{\boldsymbol{k}^2_F}}$ to linear order in q_r and quadratic order in q_t, the momentum integral in Eq. (5·10) can be carried out explicitly. For $\xi^{-1}(T) \ll m^t_{\boldsymbol{k}_F} v_{\boldsymbol{k}_F}$, one finds[17]

$$\gamma^{\mathrm{tr}}_{\boldsymbol{k}_F} = \frac{|g|}{\pi \xi_0^2}\, m^t_{\boldsymbol{k}_F} \arctan\left(\frac{q_c}{2m^t_{\boldsymbol{k}_F} v_{\boldsymbol{k}_F}}\right) K_{\boldsymbol{k}_F} d^2_{\boldsymbol{k}_F}\, T\ , \tag{5·12}$$

where q_c is a momentum cutoff and

$$K_{\boldsymbol{k}_F} = \frac{1}{2v^2_{\boldsymbol{k}}} \left(\frac{\boldsymbol{v}_{\boldsymbol{k}} \cdot \partial_{k_r} \boldsymbol{v}_{\boldsymbol{k}}}{v_{\boldsymbol{k}}\, m^t_{\boldsymbol{k}}} - \boldsymbol{v}_{\boldsymbol{k}} \cdot \partial^2_{k_t} \boldsymbol{v}_{\boldsymbol{k}}\right)\Bigg|_{\boldsymbol{k} = \boldsymbol{k}_F} . \tag{5·13}$$

The scattering rate $\gamma^{\mathrm{tr}}_{\boldsymbol{k}_F}$ is thus *linear* in T at low temperatures. Note that the correlation length $\xi(T)$ does not appear in the asymptotic low temperature behavior of $\gamma^{\mathrm{tr}}_{\boldsymbol{k}_F}$. By contrast, in the Fermi liquid regime close to the quantum critical point $\gamma^{\mathrm{tr}}_{\boldsymbol{k}_F}$ is proportional to $\xi^2 T^2 \log T$, where $\xi = \xi(T \to 0)$.[38),39)]

The prefactor of the T-linear behavior of $\gamma^{\mathrm{tr}}_{\boldsymbol{k}_F}$ varies strongly along the Fermi surface and vanishes on the Brillouin zone diagonal. This is reminiscent of the *cold spot* scenario of transport in cuprates.[40)] Inserting $\gamma^{\mathrm{tr}}_{\boldsymbol{k}_F}$ from (5·12) in Eq. (5·11) for the conductivity one runs into a divergent Fermi surface integral, due to the zeros of $\gamma^{\mathrm{tr}}_{\boldsymbol{k}_F}$ at the cold spots $\boldsymbol{k}^c_F$, leading to an infinite conductivity. However, other (than d-wave forward scattering) residual interactions will lead at least to the conventional Fermi liquid decay rate of order T^2 all over the Fermi surface, including the cold

spots. Including a Fermi liquid contribution of order T^2, the scattering rate acquires the form

$$\gamma^{\rm tr}_{\boldsymbol{k}_F}(T) = a_{\boldsymbol{k}_F} T^2 + b_{\boldsymbol{k}_F} d^2_{\boldsymbol{k}_F} T\,, \tag{5·14}$$

where the coefficients $a_{\boldsymbol{k}_F}$ and $b_{\boldsymbol{k}_F}$ are finite for all $\boldsymbol{k}_F$. Inserting this ansatz into Eq. (5·11), one obtains the resistivity[17)]

$$\rho(T) = \frac{2\pi}{e^2} \frac{\sqrt{a_{\boldsymbol{k}^c_F} b_{\boldsymbol{k}^c_F}}}{v_{\boldsymbol{k}^c_F}} T^{3/2} \tag{5·15}$$

for low T. This result for $\rho(T)$ is reminiscent of the puzzling $T^{3/2}$-behavior of the resistivity observed in overdoped $La_{2-x}Sr_xCuO_4$.[41)]

In the presence of impurities, the scattering rate has the form $\gamma^{\rm tr}_{\boldsymbol{k}_F}(T) = \gamma^{\rm imp}_{\boldsymbol{k}_F} + b_{\boldsymbol{k}_F} d^2_{\boldsymbol{k}_F} T$, for temperatures low enough that the Fermi liquid term of order T^2 can be neglected compared to the impurity term. For $T \to 0$ one then obtains a finite residual resistivity determined by impurity scattering. For low finite temperatures the resistivity increases linearly with T at low temperatures $T \ll \gamma^{\rm imp}_{\boldsymbol{k}_F}/b_{\boldsymbol{k}_F}$.

§6. Conclusions

Critical fluctuations in the vicinity of a d-wave Pomeranchuk instability in a two-dimensional electron system provide an interesting route to non-Fermi liquid behavior. The fluctuations can be viewed as long-wavelength density fluctuations with a d-wave form factor or as d-wave fluctuations of the Fermi surface. They lead to a singularity in the dynamical d-wave density correlation function at small momenta and frequencies, and to singular forward scattering. The momentum and energy dependence of the singularity is captured essentially correctly by the random phase approximation. However, interactions of fluctuations determine the temperature dependence of the correlation length $\xi(T)$.

Single-particle excitations are strongly affected by the fluctuations. The dominant contributions to the electronic self-energy $\Sigma(\boldsymbol{k},\omega)$ generated by the singular forward scattering in the quantum critical regime are proportional to $d^2_{\boldsymbol{k}}$, where $d_{\boldsymbol{k}}$ is a form factor with d-wave symmetry, such as $\cos k_x - \cos k_y$. This leads to a strong momentum dependence of $\Sigma(\boldsymbol{k},\omega)$ along the Fermi surface. The singular contributions vanish on the Brillouin zone diagonal, and have the largest amplitude near the van Hove points. The momentum dependence of $\Sigma(\boldsymbol{k},\omega)$ perpendicular to the Fermi surface is quite weak at low temperatures.

At the quantum critical point, the self-energy scales as $|\omega|^{2/3}$ with energy. This leads to a destruction of quasi-particles near the Fermi surface except on the Brillouin zone diagonal. The dispersion of the maxima of the spectral function $A(\boldsymbol{k},\omega)$ becomes flat for momenta $\boldsymbol{k}$ near the Fermi surface away from the zone diagonal. In the quantum critical regime at $T > 0$ the self-energy can be decomposed in a "classical" and a "quantum" part with very different dependences on T and ω. The classical part is due to classical fluctuations and dominates at $\omega = 0$, where it yields a contribution proportional to $T\xi(T) \propto \sqrt{T/\log T}$ to $\mathrm{Im}\Sigma(\boldsymbol{k}_F,\omega)$. The quantum

part is generated by quantum fluctuations and obeys (ω/T)-scaling in the quantum critical regime.

The relaxation of a DC charge current is determined by classical fluctuations. The transport decay rate $\gamma^{\rm tr}_{\boldsymbol{k}_F}(T)$ is linear in temperature everywhere on the Fermi surface except at the cold spots on the Brillouin zone diagonal. For pure systems, this leads to a DC resistivity proportional to $T^{3/2}$ in the low-temperature limit. In the presence of impurities the residual impurity resistance at $T = 0$ is approached linearly at low temperatures.

To what extent could soft Fermi surfaces and critical Fermi surface fluctuations play a role in cuprate superconductors? Close to a Pomeranchuk instability of the electronic system, electronic properties can be expected to react unusually strongly to slight lattice distortions which break the symmetry of the electronic system explicitly. Such "overreactions" of electronic properties have indeed been observed early on in several cuprate compounds.[42),43)] In particular, a slight orthorhombicity of the lattice structure would lead to a relatively strong orthorhombic distortion of the Fermi surface.[44)] Recent experiments on YBCO have established a remarkably strong in-plane anisotropy of electronic and magnetic properties,[7),45),46)] although the structural anisotropy of the CuO_2-planes, which is induced indirectly by the CuO-chains between the planes in that material, is rather weak.[47)] Fermi surface softening with d-wave symmetry due to forward scattering interactions provides a natural explanation of the fairly strong in-plane anisotropy observed in YBCO.[8)] Many experimental observations, which have been attributed to static or fluctuating stripes,[6)] actually provide evidence only for a tendency to orientation, not translation, symmetry-breaking, and could therefore be described equally well by a (incipient) Pomeranchuk instability.

Fermi surface fluctuations could be at least partially responsible for the non-Fermi liquid behavior observed in the "strange metal" regime of cuprate superconductors near optimal doping. In our model calculation we have obtained a strongly anisotropic anomalously large decay rate for single-particle excitations and a flattening of the dispersion relation near the Fermi surface away from the nodal direction. The properties of single-particle excitations in various cuprate compounds have been investigated in considerable detail by numerous angular resolved photoemission experiments.[48)] Extended flat bands in the van Hove region have been observed by various groups already in the early 1990s.[49)–51)] Large anisotropic decay rates have been extracted from the linewidth of low-energy peaks in the photoemission spectra observed in optimally doped cuprates, using in particular momentum scans perpendicular to the Fermi surface at various fixed energies.[52),53)] The line shape of these scans is almost Lorentzian, which is consistent with our results. Most recent measurements indicate that the previously suggested non-Fermi liquid behavior in the nodal direction, which could not be explained by d-wave fluctuations, is not tenable any more.[54)]

Concerning transport, an anisotropic scattering rate with nodes on the Brillouin zone diagonal can very naturally account for the pronounced anisotropy between the intra- and inter-plane mobility of charge carriers, as pointed out by Ioffe and Millis[40)] in their phenomenological "cold spot" scenario. According to their idea, the

intra-plane transport is dominated by quasi-particles with a long life-time near the diagonal of the Brillouin zone, while these carriers are not available for inter-plane transport, since transverse hopping amplitudes vanish on the diagonal. Strikingly, recent measurements of the momentum resolved transport decay rate in $Tl_2Ba_2CuO_{6+\delta}$ revealed a T-linear contribution with a d-wave form factor, in addition to a less momentum dependent Fermi liquid type background,[55),56)] precisely as in our result for $\gamma^{\rm tr}_{\boldsymbol{k}_F}(T)$.*)

Acknowledgements

We would like to thank C. Castellani, A. Chubukov, C. Di Castro, P. Jakubczyk, A. Katanin, A. Rosch, P. Strack, P. Wölfle, and H. Yamase for valuable discussions.

References

1) I. J. Pomeranchuk, Sov. Phys. -JETP **8** (1958), 361.
2) H. Yamase and H. Kohno, J. Phys. Soc. Jpn. **69** (2000), 332; J. Phys. Soc. Jpn. **69** (2000), 2151.
3) C. J. Halboth and W. Metzner, Phys. Rev. Lett. **85** (2000), 5162.
4) I. Grote, E. Körding and F. Wegner, J. Low Temp. Phys. **126** (2002), 1385.
5) S. A. Kivelson, E. Fradkin and V. J. Emery, Nature **393** (1998), 550.
6) S. A. Kivelson, I. P. Bindloss, E. Fradkin, V. Oganesyan, J. M. Tranquada, A. Kapitulnik and C. Howald, Rev. Mod. Phys. **75** (2003), 1201.
7) V. Hinkov, S. Pailhes, P. Bourges, Y. Sidis, A. Ivanov, A. Kulakov, C. T. Lin, D. P. Chen, C. Bernhard and B. Keimer, Nature **430** (2004), 650.
8) H. Yamase and W. Metzner, Phys. Rev. B **73** (2006), 214517.
9) S. A. Grigera et al., Science **306** (2004), 1154.
R. A. Borzi et al., Science **315** (2007), 214.
10) C. M. Varma and L. Zhu, Phys. Rev. Lett. **96** (2006), 036405.
11) A. Neumayr and W. Metzner, Phys. Rev. B **67** (2003), 035112.
12) H. Yamase and W. Metzner, Phys. Rev. B **75** (2007), 155117.
13) M. Vojta, Y. Zhang and S. Sachdev, Phys. Rev. Lett. **85** (2000), 4940; Int. J. Mod. Phys. B **14** (2000), 3719.
14) V. Oganesyan, S. A. Kivelson and E. Fradkin, Phys. Rev. B **64** (2001), 195109.
15) W. Metzner, D. Rohe and S. Andergassen, Phys. Rev. Lett. **91** (2003), 066402.
16) L. Dell'Anna and W. Metzner, Phys. Rev. B **73** (2006), 045127.
17) L. Dell'Anna and W. Metzner, Phys. Rev. Lett. **98** (2007), 136402.
18) P. A. Frigeri, C. Honerkamp and T. M. Rice, Eur. Phys. J. B **28** (2002), 61.
19) H.-Y. Kee, E. H. Kim and C.-H. Chung, Phys. Rev. B **68** (2003), 245109.
20) I. Khavkine, C.-H. Chung, V. Oganesyan and H.-Y. Kee, Phys. Rev. B **70** (2004), 155110.
21) H. Yamase, V. Oganesyan and W. Metzner, Phys. Rev. B **72** (2005), 035114.
22) A. V. Chubokov and D. L. Maslov, Phys. Rev. B **68** (2003), 155113, and references therein.
23) A. Chubukov, private communication.
24) J. A. Hertz, Phys. Rev. B **14** (1976), 1165.
25) A. J. Millis, Phys. Rev. B **48** (1993), 7183.
26) P. Jakubczyk, P. Strack, A. A. Katanin and W. Metzner, Phys. Rev. B **77** (2008), 195120.
27) C. Castellani, C. Di Castro and M. Grilli, Phys. Rev. Lett. **75** (1995), 4650.
28) A. Chubukov, Phys. Rev. B **71** (2005), 245123.
29) P. A. Lee, Phys. Rev. Lett. **63** (1989), 680.

*) The authors of Ref. 56) suggest that the prefactor of the anisotropic contribution to the transport decay rate in our theory should decrease upon moving away from van Hove filling. This is not the case, since the coupling constant g in our model is an *effective* interaction, which should increase upon approaching the more strongly correlated regime of the phase diagram with decreasing doping.

30) B. Blok and H. Monien, Phys. Rev. B **47** (1993), 3454.
31) Y. M. Vilk and A.-M. S. Tremblay, J. de Phys. I **7** (1997), 1309.
32) Ar. Abanov, A. V. Chubukov and J. Schmalian, Adv. Phys. **52** (2003), 119.
33) A. A. Katanin, A. P. Kampf and V. Yu. Irkhin, Phys. Rev. B **71** (2005), 085105.
A. A. Katanin, Phys. Rev. B **72** (2005), 035111.
34) B. L. Altshuler, L. B. Ioffe and A. J. Millis, Phys. Rev. B **50** (1994), 14048.
35) J. Rech, C. Pepin and A. V. Chubukov, Phys. Rev. B **74** (2006), 195126.
36) See, for example, G. Rickayzen, *Green's Functions and Condensed Matter* (Academic Press, London, 1980).
37) For a detailled discussion of this point for the case of a density wave instability, see S. Caprara, M. Grilli, C. Di Castro and T. Enss, Phys. Rev. B **75** (2007), 140505(R).
38) H. v. Löhneysen, A. Rosch, M. Vojta and P. Wölfle, Rev. Mod. Phys. **79** (2007), 1015.
39) P. Wölfle and A. Rosch, J. Low Temp. Phys. **147** (2007), 165.
40) L. B. Ioffe and A. J. Millis, Phys. Rev. B **58** (1998), 11631.
41) H. Takagi et al., Phys. Rev. Lett. **69** (1992), 2975.
42) J. D. Axe, A. H. Moudden, D. Hohlwein, D. E. Cox, K. M. Mohanty, A. R. Moodenbaugh and Youwen Xu, Phys. Rev. Lett. **62** (1989), 2751.
43) B. Büchner, M. Breuer, A. Freimuth and A. P. Kampf, Phys. Rev. Lett. **73** (1994), 1841.
44) H. Yamase and H. Kohno, J. Phys. Soc. Jpn. **70** (2001), 2733; J. Phys. Soc. Jpn. **71** (2002), 1154.
45) D. H. Lu, D. L. Feng, N. P. Armitage, K. M. Shen, A. Damascelli, C. Kim, F. Ronning, Z.-X. Shen, D. A. Bonn, R. Liang, W. N. Hardy, A. I. Rykov and S. Tajima, Phys. Rev. Lett. **86** (2001), 4370.
46) Y. Ando, K. Segawa, S. Komiya and A. N. Lavrov, Phys. Rev. Lett. **88** (2002), 137005.
47) O. K. Andersen, A. I. Liechtenstein, O. Jepsen and F. Paulsen, J. Phys. Chem. Solids **56** (1995), 1573.
48) For a review on photoemission in cuprates, see A. Damascelli, Z. Hussain and Z. X. Shen, Rev. Mod. Phys. **75** (2003), 473.
49) A. A. Abrikosov, J. C. Campuzano and K. Gofron, Physica C **214** (1993), 73.
50) D. S. Dessau, Z.-X. Shen, D. M. King, D. S. Marshall, L. W. Lombardo, P. H. Dickinson, A. G. Loeser, J. DiCarlo, C.-H. Park, A. Kapitulnik and W. E. Spicer, Phys. Rev. Lett. **71** (1993), 2781.
51) K. Gofron, J. C. Campuzano, H. Ding, C. Gu, R. Liu, B. Dabrowski, B. W. Veal, W. Cramer and G. Jennings, J. Phys. Chem. Solids **54** (1993), 1193.
52) T. Valla, A. V. Fedorov, P. D. Johnson, Q. Li, G. D. Gu and N. Koshizuka, Phys. Rev. Lett. **85** (2000), 828.
53) A. Kaminski, H. M. Fretwell, M. R. Norman, M. Randeria, S. Rosenkranz, U. Chatterjee, J. C. Campuzano, J. Mesot, T. Sato, T. Takahashi, T. Terashima, M. Takano, K. Kadowaki, Z. Z. Li and H. Raffy, Phys. Rev. B **71** (2005), 014517.
54) S. Borisenko, private communication.
55) M. Abdel-Jawad, M. P. Kennett, L. Balicas, A. Carrington, A. P. Mackenzie, R. H. McKenzie and N. E. Hussey, Nature Physics **2** (2006), 821.
56) M. Abdel-Jawad, J. G. Analytis, L. Balicas, A. Carrington, J. P. H. Charmant, M. M. J. French and N. E. Hussey, Phys. Rev. Lett. **99** (2007), 107002.